Journal of Non-Newtonian Fluid Mechanics 305 (2022) 104817

Contents lists available at ScienceDirect

Journal of Non-Newtonian Fluid Mechanics

journal homepage: www.elsevier.com/locate/jnnfm

Squeeze film flow of viscoplastic Bingham fluid between non-parallel plates

Elaheh Esmaeili *, Paul Grassia, Carlos Alejandro Torres Ulloa

Department of Chemical and Process Engineering, University of Strathclyde, 75 Montrose Street, Glasgow, G1 1XJ, UK

ARTICLE INFO

Keywords:
Squeeze film flow
Viscoplastic Bingham fluid
Oldroyd number
Non-parallel plates
Lubrication theory

ABSTRACT

Squeeze film flow of a viscoplastic Bingham fluid between non-parallel plates has been analysed. It is assumed that the force applied to the plates is known, therefore, their velocity must be found, and the film thickness decreases then as time proceeds. Moreover, for non-parallel plates, the position along the plates at which flow reverses direction is found as part of the solution. In the Newtonian limit, the thickness of the gap between the plates in the parallel system never quite reaches zero at any finite time, while for the non-parallel case a finite time can be obtained when the plates touch one another at a point. In squeeze flow of a viscoplastic Bingham fluid between parallel and non-parallel plates, under a fixed applied force, a final steady film thickness can sometimes be reached. This final thickness turns out to be sensitive not just to the plate tilt angle but also to the so called Oldroyd number which is defined as the ratio between yield stress and imposed stress. Nevertheless for squeeze film flow of Bingham viscoplastic fluid between non-parallel plates, the results show that other cases exist in which the lubrication force cannot always balance the applied force, leading to the plates approaching and touching at the narrowest end of the gap. Moreover torques that develop within the system have been analysed.

1. Introduction

Squeeze film flows [1] are flows in which a material is compressed between two approaching parallel or nearly parallel plane surfaces. They have myriad applications, including in areas such as engineering, biology, food industries, rheometry devices, compression moulding, papermaking, etc. [1–4]. Squeeze film flows of Newtonian and non-Newtonian fluids have been studied experimentally, theoretically and numerically. In particular, there is a comprehensive review [4] on squeeze flow theory and its applications in which a wide variety of materials such as Newtonian, viscoelastic and viscoplastic with different boundary conditions, i.e. perfect slip, no slip and partial slip at the sample-plate interfaces have been investigated.

Squeeze flow tests can be carried out either using a specified shear rate (constant displacement rate) or a specified shear stress (constant load). Thus, results can be in the form of relations between force–height, force–time and height–time depending on how the test is done [1,2,4,5]. Assuming a no slip condition between the sample and the plates, at fixed applied force, the shear rate in the squeeze film tends to fall as time proceeds (the Newtonian case implies that in fact). For viscoelastic fluids, this then means that elastic effects are likely to become less important over time [6] (the fluids behave closer to Newtonian). On the other hand, for a pseudo-plastic power law fluid say, it implies that the effective viscosity rises as time proceeds (the flow necessarily slows down relative to a Newtonian case) [2,4].

Indeed viscoplastic materials [7–9] are of special interest in squeeze film situations [3,4,10], since they flow as a fluid when the imposed stress is bigger than the yield stress but can be treated as a plug-like solid when the imposed stress is less than the yield stress. Therefore, the squeeze film flow field for a viscoplastic fluid is often considered to be divided into two regions [11–13], yielded (fluid) and plug (unyielding) region. The surface which separates yielded and plug regions is called the yield surface [14]. During squeeze film flow under constant load, as time proceeds, the yield surface would be expected to shift so that more and more of the flow domain is in the plug region and less of it is in the yielded region, until the yielded region disappears and the flow has stopped altogether, even whilst the squeeze film can remain at a finite thickness [3,5,15].

These flows are however less simple than it might first appear. When coupled with conventional lubrication theory applicable in small aspect ratios, they lead to an apparent paradox (the so called “lubrication paradox”) [11,12,16,17]. Fig. 1 is predicted to have different horizontal velocities. Hence there is predicted to be a non-zero strain rate in the normal direction even in the (supposedly non-yielding) plug region, albeit this is of much smaller magnitude than the shear strain rate in the yielded region. The paradox has however been resolved by [18]. That analysis revealed [18,19] that the yielded region was in fact what was termed a “fully-plastic” region, in which even the dominant shear

* Corresponding author.
E-mail address: elaheh.esmaeili@strath.ac.uk (E. Esmaeili).

https://doi.org/10.1016/j.jnnfm.2022.104817
Received 29 October 2021; Received in revised form 15 April 2022; Accepted 21 April 2022
Available online 5 May 2022
0377-0257/© 2022 The Author(s). Published by Elsevier B.V. This is an open access article under the CC BY license (http://creativecommons.org/licenses/by/4.0/).

stress component exceeded the yield stress. On the other hand, the plug region was revealed to be merely a "pseudo-plug". When normal stresses (in addition to shear stresses) as well as perturbations over and above the leading order horizontal flow are taken into account, the "pseudo-plug" was found to be at a stress condition just slightly in excess of the yield stress. This then admitted the required non-zero strain rate there, which as mentioned, is smaller than the shear strain rate in the "fully-plastic" region. The "fully-plastic" and "pseudo-plug" regions were separated by what was termed a "fake yield surface". For the present work however it is sufficient to consider just the leading order horizontal flow and the pressure field that is associated with it. For simplicity then we continue to use the terminology "yielded", "plug" and "yield surface" rather than the terms "fully-plastic" "pseudo-plug" and "fake yield surface" [18,19].

As alluded to above, literature has been published on the squeeze film flow between parallel plates either with constant rate or constant load. The work done by [5], investigated the behaviour of a yield stress fluid between two parallel plates with a constant load, theoretically and experimentally. However, they have not dealt with the non-parallel plates geometry. The work of [13] meanwhile provided an asymptotic solution for the two-dimensional planar squeeze film flow of a viscoplastic medium and analytical solutions for the flow fields have been compared to numerical computations. We will make use of these solutions. Nonetheless the work done by [13] and likewise by [12], only investigated the squeeze flow of a viscoplastic fluid between parallel plates with a constant squeezing rate. This requires in particular that larger squeezing forces are applied as time proceeds, with the squeezing force needing to become arbitrarily large as the gap narrows.

Few studies have investigated non-parallel squeeze film flows. One study by [20] carried out the two-dimensional numerical simulation of the squeeze film flow of a viscoplastic fluid between two approaching circular cylinders. In another study conducted by [21], the peristaltic flow of a Herschel–Bulkley fluid is examined in an inclined tube. These studies have not however used the calculation procedure developed by [5] to establish under constant load conditions what the final state of such systems might be. Thus, in the present work, non-parallel squeeze flow of a viscoplastic Bingham fluid with an assumption of a fixed squeezing force (arguably more realistic than fixed squeezing rate which requires an ever increasing force) is developed. In the present work, the final state of the system is identified, and it is also considered how the squeezing rate varies with time (up to the final state). A number of features specific to non-parallel plates i.e. identifying the position along the plates at which flow direction reverses as well as evolution of torque, have also been described.

What has motivated the present study are applications in which a viscoplastic fluid is squeezed out of a complex shaped gap. One such example is foam-based papermaking in which a foam carrier fluid is squeezed out from a network of fibres [22]. There is no need for the fibres in the network to be aligned parallel. Often moreover, length of the fibres is significantly greater than the size of the bubbles in the foam [23], in which case it might be permitted to treat the bubbles, at least in a rough approximation, as if they were a continuum. Foam-based making is in fact a very complex system [22,24], and the problem to be solved here is admittedly just a highly idealised version of it.

The rest of this work is laid out as follows. Section 2 deals with methodology and introduces governing equations for non-parallel squeeze flow geometry. After that Section 3 deals with the results obtained from the investigated squeeze flow problem. Finally, Section 4 considers the conclusions from the present study.

2. Methodology

In what follows, Section 2.1 describes the squeeze film flow problem between non-parallel plates, Section 2.2 deals with torques and Section 2.3 considers final steady states. Following that, yield stress contributions to force and torque are discussed in Section 2.4.

2.1. Squeeze film flow of Bingham viscoplastic fluid between non-parallel plates

This section considers the squeeze flow of viscoplastic Bingham fluid between non-parallel plates. The analysis for a parallel, Newtonian squeeze film is well known in the literature [25]. However for completeness we have presented it in section S1 of the supplementary material. Moreover, the behaviour of a Newtonian fluid squeezed between non-parallel plates is reviewed in section S2 to facilitate comparison with the non-parallel viscoplastic Bingham case, particularly with regard to possible final states. The solution of squeeze film flow of a Bingham viscoplastic in the parallel case has been investigated by [5] and we provide the mathematical procedure in the supplementary material, section S3 again to support the non-parallel plate case in the present section.

In what follows, standard lubrication theory assumptions [25], i.e. planar geometry, thin geometry, incompressible fluid, negligible gravity, negligible inertia, no slip boundaries are considered to apply. We consider a gap of initial thickness $\hat{H}_{c_0}$ at the centre of the plates of length $2\hat{L}$. In Fig. 1 the top plate is moving downward with a time-varying velocity $\hat{v}_{top}$ under a constant applied force $\hat{F}_{app}$ (per unit distance transverse to the two-dimensional plane) thereby displacing the fluid, while the bottom plate is stationary. Moreover θ is the angle between the upper surface and the horizontal coordinate (it is assumed that the angle θ is small).

Governing lubrication equations [16] for a viscoplastic Bingham fluid are

$$-\partial\hat{p}/\partial\hat{x} + \partial\hat{\tau}_{xy}/\partial\hat{y} = 0 \tag{1}$$

$$\partial\hat{p}/\partial\hat{y} = 0 \tag{2}$$

$$\partial\hat{u}/\partial\hat{x} + \partial\hat{v}/\partial\hat{y} = 0. \tag{3}$$

Here $\hat{u}$ and $\hat{v}$ are velocities in $\hat{x}$ and $\hat{y}$ directions, $\hat{p}$ is pressure and $\hat{\tau}_{xy}$ denotes shear stress of the viscoplastic Bingham fluid which satisfies (see e.g. [9])

$$\begin{cases} \hat{\tau}_{xy} = \pm\tau_0 + \mu\hat{\dot{\gamma}} & \text{for} \quad |\hat{\tau}_{xy}| > \tau_0 \\ \hat{\dot{\gamma}} = 0 & \text{for} \quad |\hat{\tau}_{xy}| \leqslant \tau_0. \end{cases} \tag{4}$$

Here τ_0 is yield stress, $\hat{\dot{\gamma}} = \partial\hat{u}/\partial\hat{y}$ is shear rate and μ is fluid viscosity after yielding occurs. Here the $\pm\tau_0$ term is positive if $\hat{\dot{\gamma}} > 0$ and it is negative if $\hat{\dot{\gamma}} < 0$. The dimensional variables are denoted with a hat symbol and their dimensionless analogues (described later on) will have the hat symbol dropped.

2.1.1. Non-dimensionalisation of equations

We cast equations in dimensionless form. Horizontal lengths are scaled by $\hat{L}$, and vertical lengths are scaled by $\hat{H}_{c_0}$. Horizontal velocities are scaled by $\tilde{u} \equiv (\hat{F}_{app}/\mu)(\hat{H}_{c_0}^2/L^2)$, and vertical velocities are scaled by $\tilde{v} \equiv \hat{H}_{c_0}\tilde{u}/\hat{L}$. Times are scaled by $H_{c_0}/\tilde{v} \equiv \hat{L}/\tilde{u}$. Finally pressures are scaled by $\hat{F}_{app}/\hat{L}$: note that this has the correct units of pressure since $\hat{F}_{app}$ is taken as applied force per unit distance transverse to the two-dimensional calculation domain.

The dimensionless film thickness H is a function of both time t and x coordinate. We define δ as a rescaled angle, $\delta = \theta\hat{L}/\hat{H}_{c_0}$. Geometrically δ is the thickness change between the middle of the plate and one of the ends divided by the initial thickness in the middle. Thus, the dimensionless squeeze film thickness which varies with x-coordinate and time t, can be determined

$$H(x,t) = H_c(t) - \delta\, x \tag{5}$$

where $H_c(t)$ is film thickness at the centre of the plates.

We can define a dimensionless group, the Oldroyd number (Od) which represents the relative importance of yield stress effects and

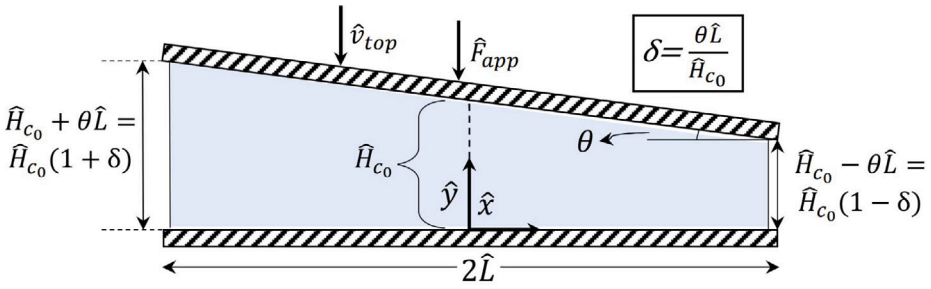

Fig. 1. Geometry of squeeze film flow between non-parallel plates.

imposed stress [14]. In our system, Oldroyd number can be defined as follows

$$Od = \frac{\text{Yield stress}}{\text{Imposed stress}} = \frac{\tau_0 \hat{L}^2}{\hat{H}_{c_0}\hat{F}_{app}}. \tag{6}$$

Suppose we make shear rate $\hat{\dot{\gamma}} \equiv \partial\hat{u}/\partial\hat{y}$ dimensionless on the scale $\tilde{u}/\hat{H}_{c_0}$ and shear stress $\hat{\tau}_{xy}$ dimensionless on the scale $\mu\tilde{u}/\hat{H}_{c_0}$. We deduce a dimensionless analogue of the constitutive equation

$$\begin{cases} \tau_{xy} = \pm Od + \dot{\gamma} & \text{for} \quad |\tau_{xy}| > Od \\ \dot{\gamma} = 0 & \text{for} \quad |\tau_{xy}| \leqslant Od. \end{cases} \tag{7}$$

Here the $\pm Od$ term is positive if $\dot{\gamma} > 0$ and is negative if $\dot{\gamma} < 0$. Recasting Eq. (1) in dimensionless form, integrating, and applying the boundary condition in which at $y = H(x,t)/2$, we have $\tau_{xy} = 0$, shear stress can be written, at least in regions in which the fluid is yielding, as below

$$\tau_{xy} = \frac{\partial p}{\partial x}\left(y - \frac{H(x,t)}{2}\right) = \pm Od + \dot{\gamma} = \pm Od + \frac{\partial u}{\partial y}. \tag{8}$$

In the non-parallel geometry, the point along the plates at which flow reverses such that the flow rate to either right or left is zero needs to be determined. This point will be denoted as x_c. The domain for solving the problem is divided into two sections $x > x_c$ and $x < x_c$ and we consider these in what follows.

2.1.2. Squeeze film flow for domain $x > x_c$

For the domain in which $x > x_c$, considering the fact that at the yield surface (denoted $y = y_{plug}$), shear rate is zero and shear stress is Od, using Eq. (8), pressure gradient with respect to x will be found

$$\frac{\partial p}{\partial x} = \frac{Od}{\left(y_{plug} - \frac{H(x,t)}{2}\right)}. \tag{9}$$

By substitution of Eq. (9) into (8), and from the Bingham fluid rheology, it is found that (in the yielded region $0 \leq y \leq y_{plug}$), $\tau_{xy} = \partial u/\partial y + Od$, thus, integrating and using the boundary condition in which at $y = 0$, $u = 0$, the velocity profile in the x direction for yielded and plug regions will be obtained.

$$\begin{cases} u = \dfrac{Od}{2(y_{plug} - \frac{H(x,t)}{2})}y^2 - \dfrac{Od}{(y_{plug} - \frac{H(x,t)}{2})}y_{plug}y & \text{for} \quad y \leqslant y_{plug} \\ u_{plug} = -\dfrac{Od}{2(y_{plug} - \frac{H(x,t)}{2})}y_{plug}^2 & \text{for} \quad y_{plug} < y < \dfrac{H}{2}. \end{cases} \tag{10}$$

The equation for flow rate Q established from the velocity profile for both plug and yielded regions is as follows

$$Q \equiv 2\left(\int_0^{y_{plug}} u\,\mathrm{d}y + \int_{y_{plug}}^{\frac{H(x,t)}{2}} u_{plug}\,\mathrm{d}y\right) = v_{top}(x - x_c). \tag{11}$$

Substitution of Eq. (10) into (11), taking the integral and making some manipulations, the final equation for y_{plug} for the domain $x > x_c$ will be generated. If $H(x,t)$ is substituted using Eq. (5) a cubic equation for y_{plug} now results

$$y_{plug}^3 - \frac{3}{2}(H_c(t) - \delta x)y_{plug}^2 - 3\frac{v_{top}(x - x_c)}{Od}y_{plug} + \frac{3}{2}\frac{v_{top}(H_c(t) - \delta x)(x - x_c)}{Od} = 0. \tag{12}$$

2.1.3. Squeeze film flow for domain $x < x_c$

In the domain, $x < x_c$, the flow and the shear stress have opposite sign from what they have for $x > x_c$. Working through the computation, we deduce

$$y_{plug}^3 - \frac{3}{2}(H_c(t) - \delta x)y_{plug}^2 + 3\frac{v_{top}(x - x_c)}{Od}y_{plug} - \frac{3}{2}\frac{v_{top}(H_c(t) - \delta x)(x - x_c)}{Od} = 0. \tag{13}$$

2.1.4. Solving for y_{plug}

The next step is to solve for the yield surface, y_{plug}, which is a function of position x, based on the two obtained Eqs. (12) and (13) for domains $x > x_c$ and $x < x_c$ respectively. To do so, a standard numerical method such as the Newton–Raphson technique is employed. Following an analogous procedure to that used for parallel plates (discussed in the supplementary material, section S3.1), assuming small values of $|x - x_c|$ and y_{plug}, a first guess for y_{plug} can be obtained. Specifically, based on the observation that at $x = x_c$ there can be no fluid motion either to left or right, hence there is no strain rate $\partial u/\partial y$ at any y. Hence at $x = x_c$, we must have $y_{plug} = 0$. For the domain $x > x_c$ but close to $x = x_c$, it follows that y_{plug} must be small, i.e. $y_{plug} \ll H(x,t)/2$. The integral within (11) then evaluates to $u_{plug}H(x,t)$ which we set equal to $v_{top}(x - x_c)$, with $u_{plug} \approx y_{plug}^2 Od/H(x,t)$ via (10). We can use analogous assumptions for the domain $x < x_c$, therefore, the initial guess for y_{plug} is

$$\begin{cases} y_{plug} = \sqrt{v_{top}(x - x_c)/Od} & \text{for} \quad x > x_c \\ y_{plug} = \sqrt{v_{top}(x_c - x)/Od} & \text{for} \quad x < x_c. \end{cases} \tag{14}$$

These only apply if they predict $y_{plug} \ll H(x,t)/2$. More generally we can have y_{plug} values up to $H(x,t)/2$. Nevertheless once we have the correct y_{plug} value at any given x, we can readily find it at a nearby x, using one y_{plug} value as an initial guess for the next. We end up with y_{plug} values for all x, provided H_c, v_{top} and x_c are given, and provided Od and δ are specified. The technique for finding v_{top}, x_c and ultimately squeeze film thickness H versus time t is described next.

2.1.5. Computing film thickness versus time

So far, the computational procedure for the constant load and constant rate systems have been similar. In this section, we proceed to find the force as a function of velocity, and hence the velocity required to deliver a constant load, and so we start to see a deviation between the constant load and constant rate systems.

Now, after finding y_{plug}, for the domain $x > x_c$, we have

$$p = \int_x^1 \frac{Od}{\frac{H(x,t)}{2} - y_{plug}}\,\mathrm{d}x. \tag{15}$$

Meanwhile for $x < x_c$ we have

$$p = \int_{-1}^{x} \frac{Od}{\frac{H(x,t)}{2} - y_{plug}}\,\mathrm{d}x. \tag{16}$$

The value of x_c needs to be chosen to ensure p is continuous at $x = x_c$. Once that is achieved (for any selected v_{top}) the value of v_{top} needs to be chosen to ensure $\int_{-1}^{1} p(x)\,\mathrm{d}x = 1$, the integral being readily computed numerically by quadrature. All this says is that in the dimensionless system considered here, the constant load is set to unity. We then evolve $H_c(t)$ according to $\mathrm{d}H_c(t)/\mathrm{d}t = -v_{top}$, with $H(x,t)$ then given by Eq. (5). To start the iteration at initial time, we need guesses of x_c and v_{top}. However we have guesses corresponding to the Newtonian case (see equations (S17) and (S18) in the supplementary material), and in general we expect that the Newtonian v_{top} provides an upper bound for the velocity in the viscoplastic Bingham fluid case. Once we have x_c and v_{top} values initially, we can then use x_c and v_{top} values at one time step as initial guesses for the subsequent time step.

2.2. Computing torque

In addition to computing film thickness versus time, the numerical scheme outlined above also allows us to track another quantity namely torque T. The scheme balances a lubrication force developed between the plates to an external applied force (which as mentioned is unity in the dimensionless system). However if the plates are tilted, a lubrication torque also develops and to keep the tilt angle fixed (as is assumed here) an external applied torque would be needed to balance it. We can however quantify the lubrication torque (per unit distance normal out of the two-dimensional plane) via $T = \int_{-1}^{1} x\,p(x)\,\mathrm{d}x$. Since p versus x is computed numerically at any instant in time, this torque can also be evaluated by quadrature.

The question we now ask is whether the plates ever come to rest at a finite film thickness (as is known to happen for a viscoplastic Bingham fluid in a parallel plate geometry as described in supplementary material section S3) or whether their right hand ends manage to touch (as happens for a Newtonian fluid between non-parallel plates as demonstrated in section S2). The question is addressed in the next section.

2.3. Steady state for viscoplastic Bingham fluid between non-parallel plates

This section develops the steady state solution for the system. The analogous approach for a yield stress fluid system in a parallel plate configuration is provided in section S3 and more specifically in section S3.4 of the supplementary material. In the parallel plate system, a steady state with a finite gap thickness is always found to exist. However in a non-parallel plate system, a steady state with a finite gap does not always exist. If there is no such steady state, then the plates eventually touch.

2.3.1. Conditions for steady state to exist

In the final state, the plug region fills the entire gap and the yield surface is at $y_{plug} = 0$. On the yield surface, there is a point now denoted $x = x_{cf}$ at which the dimensionless shear stress changes sign from $-Od$ to $+Od$. This x_{cf} is the final value of x_c (which typically denotes the point at which flow changes sign). However there is no flow at all in the final state, so what changes sign is now the shear stress.

We integrate the equation $\partial p/\partial x = \mp Od/((H_{cf} - \delta\,x)/2)$ applicable in the final steady state. Here H_{cf} is the assumed final thickness at the centre of the plates. Thus for $x > x_{cf}$, the pressure profile is determined

$$p(x) = \frac{2Od}{\delta}\ln\frac{H_{cf} - \delta x}{H_{cf} - \delta}. \tag{17}$$

For $x < x_{cf}$, the pressure profile is

$$p(x) = \frac{2Od}{\delta}\ln\frac{H_{cf} + \delta}{H_{cf} - \delta x}. \tag{18}$$

Since the pressure profile has to be continuous at $x = x_{cf}$, Eqs. (17) and (18) should be equal at this point

$$\frac{2Od}{\delta}\ln\frac{H_{cf} - \delta x_{cf}}{H_{cf} - \delta} = \frac{2Od}{\delta}\ln\frac{H_{cf} + \delta}{H_{cf} - \delta x_{cf}}. \tag{19}$$

Simplifying Eq. (19), a quadratic equation can be obtained

$$x_{cf}^2 - 2\frac{H_{cf}}{\delta}x_{cf} + 1 = 0. \tag{20}$$

Solving the quadratic Eq. (20) gives x_{cf} as a function of H_{cf} and δ

$$x_{cf} = \frac{H_{cf}}{\delta} - \sqrt{\frac{H_{cf}^2}{\delta^2} - 1}. \tag{21}$$

The force applied over the entire plate length can be calculated utilising the pressure profiles obtained above

$$\begin{aligned} F &= \int_{-1}^{x_{cf}} p(x)\mathrm{d}x + \int_{x_{cf}}^{1} p(x)\mathrm{d}x \\ &= \frac{2Od}{\delta}\left(\left(x_{cf} - \frac{H_{cf}}{\delta}\right)\ln\frac{H_{cf}^2 - \delta^2}{(H_{cf} - \delta x_{cf})^2} + 2x_{cf}\right). \end{aligned} \tag{22}$$

Substituting the obtained x_{cf} from Eq. (21) into (22), considerable simplification results, because the argument of the logarithmic term turns out to be unity, so the logarithm itself vanishes. Assuming the plates have stopped moving then, the force applied over the entire plate length turns out to be

$$F = 4\frac{Od}{\delta}\left(\frac{H_{cf}}{\delta} - \sqrt{\frac{H_{cf}^2}{\delta^2} - 1}\right) = \frac{4Od}{\delta}x_{cf}. \tag{23}$$

This force generated by the pressure profile must now be matched to the unit force applied to the plates, and conditions determined in which physically meaningful solutions for H_{cf} or equivalently for x_{cf} are obtained. Setting $F = 1$ we need to find combinations of Od and δ that admit solutions with $H_{cf} > \delta$ or equivalently with $x_{cf} < 1$. It is clear that to achieve this we require $4Od/\delta > 1$. Provided this condition is satisfied, the gap at the right hand end $H_{cf} - \delta$ is then finite.

2.3.2. Final steady state torque calculation

As well as computing a force in the steady state, we can also compute a torque. For a Bingham fluid in a non-parallel system this can be obtained by taking the integral $\int_{-1}^{1} x\,p(x)\,\mathrm{d}x$ using pressure profiles provided in Eqs. (17) and (18). For comparison, analysis of torque for a Newtonian fluid (albeit at unsteady state) has been done in the supplementary material, section S2.2, but here we focus on the steady Bingham case. We find

$$\begin{aligned} T_{steady} = \frac{Od}{2\delta^3}\Bigg(&2(H_{cf}^2 - \delta^2 x_{cf}^2)\ln\frac{(H_{cf} - \delta\,x_{cf})^2}{H_{cf}^2 - \delta^2} \\ &+ 4\,\delta\,x_{cf}H_{cf} + 2\delta^2(x_{cf}^2 - 1)\Bigg) \end{aligned} \tag{24}$$

where T_{steady} is the steady state torque and x_{cf} is a known function of H_{cf}/δ from Eq. (21). As before the logarithmic term vanishes (its argument is unity) and after some further algebra using Eq. (20), the steady state torque reduces to

$$T_{steady} = \frac{2Od}{\delta}x_{cf}^2. \tag{25}$$

However, from Eq. (23) in the final steady state we already know $(Od/\delta)x_{cf} = \frac{1}{4}$. Hence final torque is

$$T_{final} = x_{cf}/2. \tag{26}$$

This indicates that T_{final} depends on the film thickness at the right hand end $H_{cf} - \delta$ relative to the film thickness at the centre H_{cf}. For instance, a final state with a gap on the right hand end that is not too narrow relative to the centre (i.e. small δ/H_{cf}, hence small x_{cf}) leads to small

T_{final}. However a much narrower gap with plates almost touching when they stop (i.e. δ/H_{cf} close to unity, hence x_{cf} close to unity) leads to $T_{final} = \frac{1}{2}$. Note that this is only half the torque of the Newtonian system when it touches (see section S2.2 in supplementary material).

There is another way to interpret the torque obtained in Eq. (25). Rather than obtaining it at the final steady thickness H_{cf}, we can find torque at any instantaneous H_c. This allows us to estimate (at any instant) a yield stress contribution to both force and torque, the total force and torque being a sum of yield stress contributions and viscous contributions. This approach will be discussed in Section 2.4. However, when a steady state is reached, there is no motion, hence no viscous contribution, and so total force and torque arise entirely from yield stress contributions.

2.3.3. Maximum and minimum Oldroyd number

To proceed we next define a parameter called η which involves the ratio between the tilt angle and the Oldroyd number

$$\eta = \delta/(4Od). \tag{27}$$

Note that the bracketed term in Eq. (23) is always less than unity for any $H_{cf}/\delta > 1$, i.e. $x_{cf} < 1$ always. Hence in order to satisfy the constraint $F = 1$, it is essential to have $\eta < 1$. In other words for a specified Od there is a maximum δ at which a steady state solution with a finite thickness could exist (or equivalently for any δ, there is a minimum Oldroyd number, Od_{min}, for a steady state with a finite thickness to exist)

$$Od_{min} = \delta/4. \tag{28}$$

If $Od < Od_{min}$, the plates rather than reaching steady state instead must touch as they do in the Newtonian limit $Od \to 0$. It is only in the limit of parallel plates with $\delta \to 0$ that Od_{min} falls to zero. When plates are tilted, the narrow end of the gap is more effective at supplying force to the plates than the wider end is. The issue with increasing δ however is that the gap only remains narrow over a limited domain of x close to its right hand end. An increase in δ therefore must be accompanied by an increase in Od (effectively an increase in yield stress of the fluid) to ensure that Eq. (23) in the absence of any fluid motion is still able to satisfy $F = 1$.

If $\eta > 1$, there is no steady state in which the yield stresses in the fluid are able to balance the imposed unit force on the plates. The plates must always keep moving until their right hand ends touch, as happens in the Newtonian limit for instance. Moving plates always have $y_{plug} > 0$, and this leads to larger pressures p and larger forces F (due to those pressures) than a stationary plate case can deliver (via Eq. (23)). Hence moving plates can achieve $F = 1$ even with $\eta > 1$ even though stationary plates cannot.

In addition to Od_{min} given above, there is a maximum Oldroyd number, Od_{max}, at which $H_{cf} = 1$: at this Od_{max}, the plates will not move at all. Inserting $H_{cf} = 1$ in Eq. (23) and rearranging, Od_{max} which depends on δ turns out to be

$$Od_{max} = \frac{1 + \sqrt{1 - \delta^2}}{4}. \tag{29}$$

2.3.4. Phase diagram for permitted states of system

Fig. 2 shows the phase diagram in the Od versus δ plane in which there are three regions, "do not move"; "move and stop"; "move and touch". Although (at any fixed δ) there is both a Od_{min} and Od_{max} for the plates to move and stop, in the case of fixed Od, there is only a maximum δ value, δ_{max} say. However what happens at that δ_{max} depends on the value of Od. If $Od < \frac{1}{4}$, then δ_{max} corresponds to the plates moving and touching. However if $Od > \frac{1}{4}$, then δ_{max} corresponds to the plates not moving at all.

Generally speaking, the data for the unsteady state evolution are sensitive to both δ and Od number. However the final fate of the system (i.e. whether the plates stop without touching or whether instead they move and touch) is only dependent on the η value. Indeed, if $\eta < 1$, such that the final film thickness is non-zero, the final state is approached but an arbitrarily long time is needed to reach it at least in principle (qualitatively this is similar to the viscoplastic Bingham case in a parallel system). However, if $\eta > 1$, the gap falls to zero at the right hand end and a non-parallel viscoplastic Bingham system will behave instead more like a Newtonian non-parallel case. In the Newtonian case, the right hand ends of the plates touch in a finite time (see section S2).

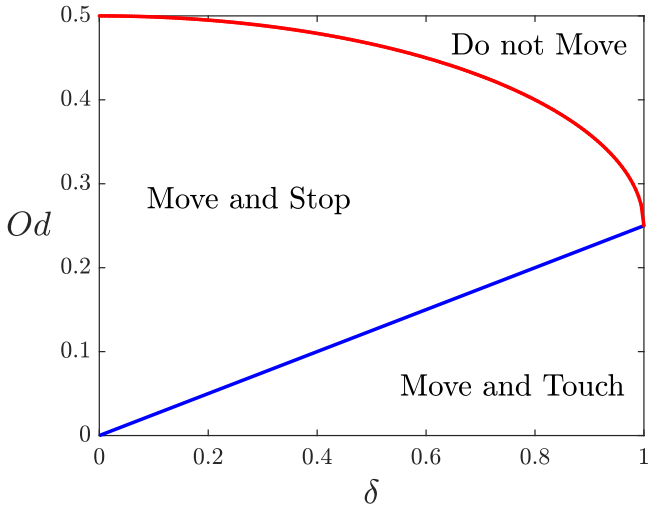

Fig. 2. Phase diagram in the Od vs δ plane for squeeze flow of viscoplastic Bingham fluid between non-parallel plates. In the "move and stop" and "do not move" regions, $\eta < 1$. In the "move and touch" region, $\eta > 1$.

2.3.5. Computing final film thickness

Having now identified the domain for which steady solutions are possible, we proceed to analyse the steady solutions further. Returning to Eq. (23) assuming $\eta < 1$, and imposing $F = 1$ we deduce

$$H_{cf} = \frac{\delta^2}{8Od} + 2Od. \tag{30}$$

For any Od number less than the maximum, a final H_{cf} less than unity can be determined. Now using this H_{cf} value, the point x_{cf} at which the viscoplastic stress switches sign can be defined. This can be determined via Eq. (21) and/or (23), and the result is

$$x_{cf} = \delta/(4Od) \equiv \eta. \tag{31}$$

Note that this steady state viscoplastic x_{cf} in general differs from the instantaneous Newtonian x_c given by Eq. (S17). Note also that as $\eta \to 1$, meaning the plates almost touch at their right hand ends once they have stopped moving, we find that $x_{cf} \to 1$, i.e. shearing in the final state is entirely towards the left. Furthermore, as already mentioned, in the non-parallel case torques can develop, and it turns out that final states with the largest x_{cf} also exhibit the largest torques. Indeed based on Eq. (26), torque is just $x_{cf}/2 = \eta/2$.

Rearranging Eq. (30) in terms of η gives $H_{cf}/(2Od)$ which is the average film thickness in the final state (at the centre of the plates) relative to the parallel case. This satisfies

$$\frac{H_{cf}}{2Od} = \eta^2 + 1. \tag{32}$$

Another important quantity, $(H_{cf} - \delta)/2Od$, which is the minimum film thickness (at the right hand end) in the final state relative to the parallel case, can be obtained

$$\frac{H_{cf} - \delta}{2Od} = (1 - \eta)^2. \tag{33}$$

The ratio between Eq. (33) and Eq. (32), $(H_{cf} - \delta)/H_{cf}$, is a measure of uniformity or otherwise of gap thicknesses such that it is zero if

polydisperse (the gaps at either end of the plates have different sizes) and unity if monodisperse (the gaps at either end have, in relative terms at least, the same thickness)

$$\frac{H_{cf}-\delta}{H_{cf}} = \frac{(1-\eta)^2}{\eta^2+1}. \tag{34}$$

To summarise Eqs. (32) and (33) give final film thicknesses in a tilted case relative to a parallel one. Meanwhile Eq. (34) tells us about the uniformity of final film thicknesses in the tilted case. These quantities depend on η, but not on Od and δ individually.

2.4. Yield force and yield torque calculation

For the Bingham parallel system presented in section S3.3 of supplementary material, we discuss a so called "yield force" contribution to the total force (the remainder of the total force being viscous force). The yield force is the force that would be developed with a given plate separation in the hypothetical case in which motion is stopped. Typically early on in the evolution, when plate separations are still quite large, yield force can be relatively small, meaning that total force is primarily viscous. However (see e.g. Figure S8) we show that over time eventually all the force becomes yield force. In this present section we explore the analogous behaviour for the non-parallel system.

Of course in the non-parallel case, in addition to defining a "yield force", we can also define a "yield torque". Again these both correspond at any given plate separation to the situation that occurs in the hypothetical case in which motion is stopped. The formulae we need are just (23) and (25), but using now the instantaneous H_c, albeit still computing x_c for this H_c value using (21). Of course the yield force and yield torque are not the same as the total force and total torque, since the totals include viscous contributions as well. Typically we can expect the yield force and yield torque to start out quite small, and only grow to match the total force and total torque in a situation in which the plates move and stop. On the other hand, if the plates instead move and touch (which can happen in a non-parallel system but not a parallel one), the yield force and yield torque might never match the total force and total torque.

3. Results and discussion

In the present section, results for a viscoplastic Bingham fluid in a non-parallel plate scenario are presented. We consider yield surfaces (Section 3.1), film thicknesses (Section 3.2), forces (Section 3.3), torques (Section 3.4) and final steady states (Section 3.5). The supplementary material, sections S4 and S5 focus primarily on results for the Newtonian fluid between parallel and non-parallel plates, and a viscoplastic Bingham fluid in a parallel plate configuration, respectively. Those results are useful for comparing and contrasting with the viscoplastic non-parallel case to be treated here, along with additional results which are presented in section S6.

3.1. Yield surface

The yield surface, y_{plug} versus x for $H_c = 1$ and $\delta = 0.2$ is shown in Fig. 3. This shows that y_{plug} for $x > x_c$ is not necessarily a monotonically increasing function of x, because y_{plug} has a maximum value of $H(x,t)/2$ and $H(x,t)$ is a decreasing function of x. Note that for $\delta = 0.2$, the maximum Od just slightly above $Od \approx 0.495$ is determined (via equation (29)). Close to this maximum Od number, y_{plug} is small.

For small Od however, y_{plug} is close to $H(x,t)/2$ (except very close to $x = x_c$ where $y_{plug} = 0$). For x just slightly greater than x_c, the value of y_{plug} increases very sharply at first (a consequence of the square root law in Eq. (14)), but for values of $Od = 0.1$ or less, y_{plug} reaches a maximum at a certain x, then, starts to decrease gradually.

The yield surface, y_{plug} versus x corresponding to $H_c = 1$ for different δ values and a constant $Od = 0.3$ is shown in Fig. 4. It is seen

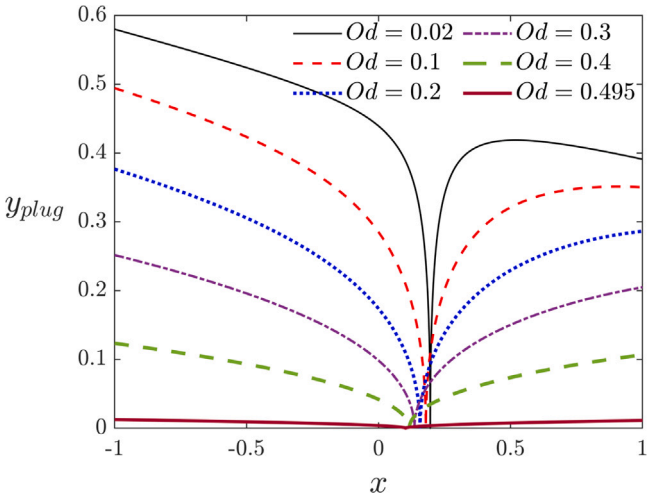

Fig. 3. Yield surfaces as functions of x corresponding to $H_c = 1$ and $\delta = 0.2$ for different Oldroyd numbers. Note that $Od = 0.495$ is close to the maximum Od number for the particular $\delta = 0.2$, so that $y_{plug} \ll 1$ when $H_c = 1$ in this case. The different Od values here have different v_{top} and x_c, values for which are reported in section S6.

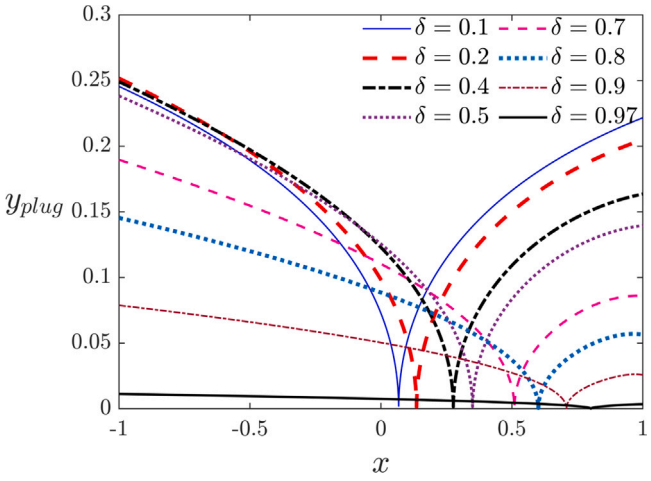

Fig. 4. Yield surfaces as functions of x corresponding to $H_c = 1$ and $Od = 0.3$ for different δ values. The different δ values here have different v_{top} and x_c, values for which are reported in section S6.

that, by increasing δ, the value of x_c increases and the yield surface becomes increasingly asymmetrical, tending to be thicker on the left hand side and thinner on the right hand side due to the geometrical constraint. For even larger δ however, y_{plug} can be small even on the left hand side, despite the wider gap there. This is due to v_{top} turning out to be small for these larger δ. Indeed by rearranging equation (29), a maximum value of δ (for the plates to move at all) just above 0.97 can be obtained for $Od = 0.3$.

Note that Figs. 3 and 4 tell us the locations of the plug region and yielded region, but not the velocities within each of those regions. Data for these velocities are however reported in section S6 in supplementary material.

Note moreover that Figs. 3 and 4 just consider one instant of time, i.e. the initial instant at which $H_c = 1$. The shapes of the yield surfaces can also be computed at later times with $H_c < 1$. However results are not presented here, because qualitatively the shapes are similar to those already seen in Figs. 3 and 4. The narrower the gap, the more impact the yield stress has upon the system, to the point that motion might stop altogether (as per Section 2.3). Hence decreasing H_c at fixed Od is similar, as far as shapes of yield surfaces are concerned, to increasing

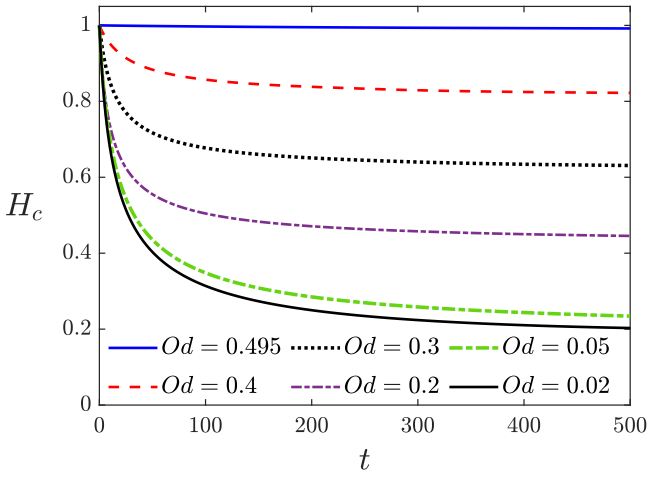

Fig. 5. Film thickness vs time for a constant $\delta = 0.2$ and different Oldroyd numbers.

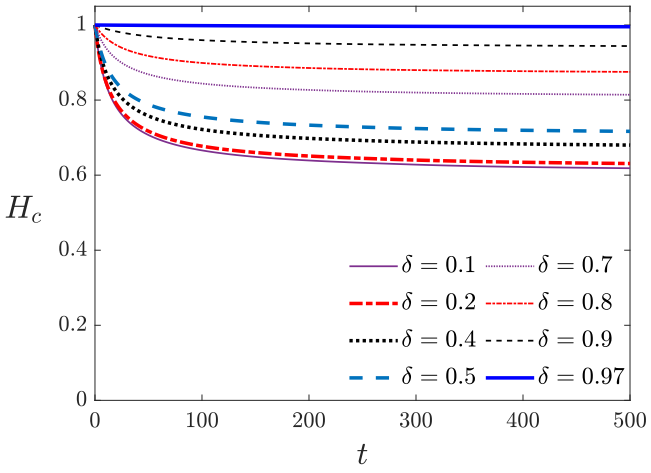

Fig. 6. Film thickness vs time corresponding to $Od = 0.3$ and different δ values.

Od at fixed H_c. Likewise the narrower the gap, the more impact a given tilt angle has upon the ratio of the film thickness between the right hand end and the centre. Hence decreasing H_c at fixed δ is similar, as far as shapes of yield surfaces are concerned, to increasing δ at fixed H_c. Instead of focussing on how y_{plug} varies with varying H_c, we therefore focus in what follows on how film thickness varies with time.

3.2. Film thickness versus time results

Changes of film thickness with respect to time for a constant $\delta = 0.2$ and various Od numbers are shown in Fig. 5. For the maximum $Od \approx 0.495$, the plates never move at all, whereas, for very small Od numbers (i.e. according to Eq. (28) for $Od < 0.05$ with this particular δ), the plates move and touch one another, and for all values of Od number in between, the plates move and stop at a final film thickness without touching one another at the right hand end. Assuming the plates move and stop without touching, Eq. (30) implies final film thickness is dependent not just on Od, but also on the ratio between tilt angle δ and Od number which appears in the definition of η in Eq. (27).

Film thickness versus time for different δ values and a constant $Od = 0.3$ is shown in Fig. 6. As δ increases, the final thickness H_{cf} increases. For any value of Od, there is a maximum value of δ beyond which the system stops moving. Using Eq. (29), the maximum δ value for a given Od number can be estimated (i.e. for $Od = 0.3$, a δ_{max} just slightly above 0.97 is achieved). All the δ values here are therefore less than the maximum. Hence, for all values of δ shown, the plates move, but also stop at final thickness since the value of η (see Eq. (27)) is also less than unity. However, for some cases (e.g. $\delta = 0.97$ or $\delta = 0.9$) the plates barely move before stopping.

A general comparison of film thickness versus time for squeeze film flow of a viscoplastic Bingham fluid with a constant $Od = 0.3$ between parallel non-parallel plates with different δ values is depicted in Fig. 7. In addition to that, changes of thickness at right hand ends of the plates (i.e. $H_c - \delta$) versus time for the two non-parallel cases are shown in the figure.

The difference between the final film thickness in the parallel case and the $\delta = 0.2$ non-parallel case is very small indeed, in line with the prediction of (30) which suggests this difference is second order in η and hence in δ. The difference with respect to the system with $\delta = 0.5$ is larger. Nonetheless, both the non-parallel systems shown here behave at least quantitatively analogous to the parallel case, with the gap at the right hand ends of the plates never reaching zero thickness as seen for the curves of $H_c - \delta$ (contrast this with section S4 in supplementary material and in particular Figure S3).

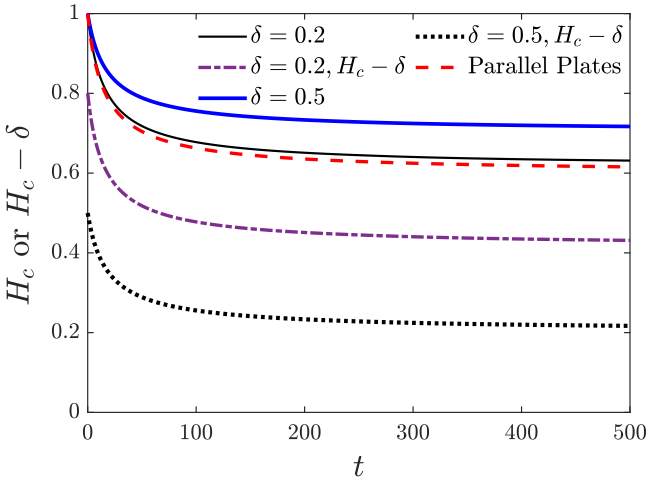

Fig. 7. Film thickness vs time corresponding to $Od = 0.3$ for parallel plates and non-parallel plates with δ values $\delta = 0.2$ and $\delta = 0.5$.

In Fig. 7 the parallel H_{cf} always lies between the non-parallel H_{cf} and the non-parallel $H_{cf} - \delta$, but is always further from the latter. This follows from Eq. (33) which suggests $H_{cf} - \delta$ is a first order quantity in η and hence first order in δ.

3.3. Contributions to the force

The force contributions (comprised of yield force and viscous force contributions summing to unity) as time proceeds for different Od values and $\delta = 0.2$ are shown in Fig. 8. The analogous result for the Bingham parallel system has been provided in the supplementary material, section S5.3.

For bigger Od numbers in the move and stop region (i.e. $Od = 0.2$, $Od = 0.1$), after relatively short times, yield force dominates the viscous force which is similar to the behaviour of the Bingham parallel system. However, for the smallest Od number considered (i.e. $Od = 0.02$) which is in the move and touch region, the yield force starts small, and despite it growing, it never approaches anywhere near unity. In fact when the plates eventually touch at right hand end of the gap the yield force can only ever reach $(4Od)/\delta$.

3.4. Torque results

Fig. 9 shows the numerically computed total torque (T; see Section 2.2) and also yield torque (T_{yield}; see Section 2.4) versus time for

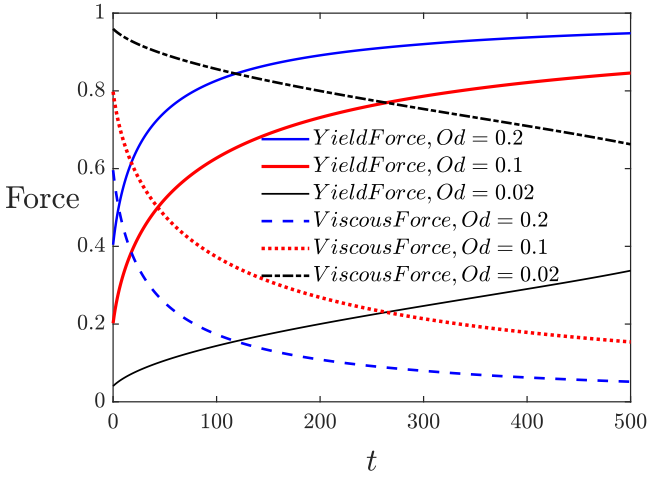

Fig. 8. Force contributions to the squeeze flow vs time for different Oldroyd numbers and $\delta = 0.2$ in the non-parallel geometry.

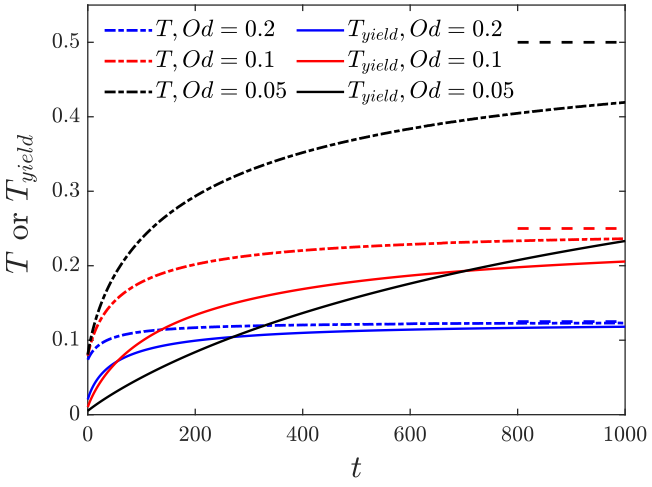

Fig. 9. Numerically computed total torque and also yield torque versus time for different Od numbers and $\delta = 0.2$. The horizontal dashed lines are the final torques attained in the limit of long times.

different Od numbers and a constant $\delta = 0.2$. From the figure, for each Od value the total torque is bigger than the yield torque and as time proceeds, the total torque and yield torque come closer together. For the largest Od number plotted (i.e. $Od = 0.2$), in fact total and yield torques are close together for almost all times. However, for the smallest Od number plotted (i.e. $Od = 0.05$), the yield torque starts off very small as mostly viscous torque is present initially and only by increasing the time, do the total and yield torques come closer together. Note that case $Od = 0.05$ with $\delta = 0.2$ has $\eta = 1$ so is on the boundary between the move and stop region and the move and touch region. Any smaller Od number will be in the move and touch region, and in such cases, the yield torque will never reach the same value as the total torque.

Another important point is that as Od decreases, the torque overall increases, whereas the yield torque starts off smaller but finishes larger due to the fact that the smaller the Od number, the greater the nonuniformity (average film thickness relative to film thickness on the right hand end) in the final state. This leads to a greater value of x_{cf}, and thus a larger final yield torque. Indeed the predicted final torque for each Od value is found via Eq. (26) and then given x_{cf} from Eq. (31), the final torque is found to be $T_{final} = \delta/(8Od)$. As seen in Fig. 9, the curves for each Od value are approaching the predicted final torque, although in the $Od = 0.05$ case, the approach is seen to be rather slow.

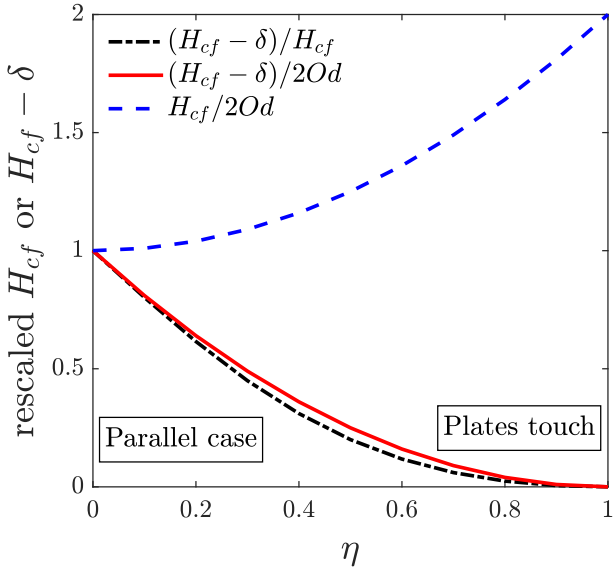

Fig. 10. Final film thicknesses in terms of $\eta = \delta/(4Od)$ values. The parallel case is $\eta = 0$ and the plates touch at $\eta = 1$.

This completes the discussion of torque in the Bingham fluid case, although a comparison between torques for Newtonian and Bingham fluids both as functions of x_c has been discussed in the supplementary material, Figure S5.

3.5. Steady states

In Fig. 10 plots are shown of $H_{cf}/(2Od)$ the average film thickness in the final steady state relative to the parallel case, $(H_{cf} - \delta)/(2Od)$ the minimum film thickness in the final state relative to the parallel case, and $(H_{cf} - \delta)/H_{cf}$ which is a measure of how uniform or nonuniform of film thicknesses are, specifically $(H_{cf} - \delta)/H_{cf}$ measures the ratio of the narrowest point to the average film thickness. All these quantities are plotted in terms of η (see Eqs. (32)–(34)), recalling that they are indeed functions only of η and not of Od and δ individually. In the case of the ratio $(H_{cf} - \delta)/H_{cf}$ in particular, note that as η increases, this ratio becomes smaller and hence the more polydisperse the system becomes in terms of film thickness, since the narrowest gap at the right hand end is then much thinner than the average thickness.

4. Conclusions

We considered a viscoplastic Bingham fluid squeezed between non-parallel plates (extending the work of [5] which considered merely the parallel geometry) under a fixed applied force (unlike the work of [13] which considered a fixed squeezing rate and parallel plates). We have also investigated the torque for the tilted plates.

Under a fixed applied force, a final film thickness can be found at which the plates stop moving. The final thickness is sensitive to Oldroyd number. A maximum Oldroyd number can be found beyond which the film thickness remains constant always without any squeezing whatsoever, due to the fact that the whole solution domain is in a plug region even at the initial instant. However, decreasing Oldroyd number allows the system to yield, and thereby reduce the film thickness as time increases. In a parallel system though, for any finite Oldroyd number, the two plates never touch even at infinite time. How the non-parallel, viscoplastic system which is considered here behaves depends, however, upon the ratio between the tilt angle, δ and the Oldroyd number, Od, this ratio appearing in the definition of a parameter $\eta \equiv \delta/(4Od)$.

If this ratio is small (i.e. $\eta < 1$), the behaviour is analogous to a viscoplastic Bingham fluid in a parallel configuration: squeezing stops while the gap is still finite. If this tilt angle to Oldroyd number ratio becomes too large (i.e. $\eta > 1$) however, the behaviour is more akin to a Newtonian fluid in a non-parallel configuration: the plates touch one another at a point. It is in the narrow part of the gap in which a viscoplastic Bingham fluid is best able to resist squeezing, but for a large tilt angle, the gap can only remain narrow over a very limited distance. Hence, with sufficient tilt, the applied force overcomes the yield stress even in the narrow part of the gap and drives the plates to touch. Moreover larger Oldroyd numbers lead to smaller η and hence more monodisperse film thicknesses.

Changing Oldroyd number also impacts on torque. Decreasing Od number increases the torque value, and torque also increases as time proceeds. In particular the torque is comprised of viscous and yield stress components. As Od decreases, the yield torque component is typically very small at early times as viscous torque dominates the yield torque. Then, as time proceeds and the system approaches a final state, the yield torque tends to dominate the viscous torque due to the fact that fluid is not moving in the final state.

Although we have managed to obtain model predictions here it is worth reflecting on the limitations of the model itself, that would also need to be overcome in future work. We have considered for simplicity a two-dimensional planar system (squeezing plates together). Squeezing together plates is however often a three-dimensional problem, as there will be many squeeze flow applications in which it is likely to be easier for fluid to escape by flowing in various directions during squeezing. Moreover we have ignored rotation of the plates. In reality the pressure field induced in the squeeze film, places not just a force on the plates (that balances the applied force) but also, as we have discussed, a torque. By balancing torque in addition to force it should be possible to deduce both a plate squeezing rate and a plate rotation rate. Rotation does however lead to a slightly more complicated flow field in the squeeze film (specifically equation (11) no longer applies). Here of course we have computed instead the torques that develop in the absence of rotation. Nevertheless the signs of those torques suggest that had rotation been permitted, it would have been such as to move the configuration closer to parallel as time evolved.

Declaration of competing interest

The authors declare that they have no known competing financial interests or personal relationships that could have appeared to influence the work reported in this paper.

Acknowledgments

The authors acknowledge support from EPSRC grant EP/V002937/1. E. Esmaeili also acknowledges support from a University of Strathclyde Student Excellence Award.

Appendix A. Supplementary sections

Supplementary material related to this article can be found online at https://doi.org/10.1016/j.jnnfm.2022.104817.

References

[1] D.F. Moore, A review of squeeze films, Wear 8 (4) (1965) 245–263.
[2] O.H. Campanella, M. Peleg, Squeezing flow viscometry for nonelastic semiliquid foods: Theory and applications, Crit. Rev. Food Sci. Nutr. 42 (3) (2002) 241–264.
[3] G.H. Meeten, Yield stress of structured fluids measured by squeeze flow, Rheol. Acta 39 (4) (2000) 399–408.
[4] J. Engmann, C. Servais, A.S. Burbidge, Squeeze flow theory and applications to rheometry: A review, J. Non-Newton. Fluid Mech. 132 (1–3) (2005) 1–27.
[5] G. Covey, B. Stanmore, Use of the parallel-plate plastometer for the characterisation of viscous fluids with a yield stress, J. Non-Newton. Fluid Mech. 8 (3–4) (1981) 249–260.
[6] G. Brindley, J.M. Davies, K. Walters, Elastico-viscous squeeze films. Part I, J. Non-Newton. Fluid Mech. 1 (1) (1976) 19–37.
[7] P. Coussot, Yield stress fluid flows: A review of experimental data, J. Non-Newton. Fluid Mech. 211 (2014) 31–49.
[8] P. Coussot, A.Y. Malkin, G. Ovarlez, Introduction: Yield stress – or 100 years of rheology, Rheol. Acta 56 (3) (2017) 161–162.
[9] D. Bonn, M.M. Denn, L. Berthier, T. Divoux, S. Manneville, Yield stress materials in soft condensed matter, Rev. Modern Phys. 89 (2017) 035005.
[10] B. Rabideau, C. Lanos, P. Coussot, An investigation of squeeze flow as a viable technique for determining the yield stress, Rheol. Acta 48 (2009) 517–526.
[11] G.G. Lipscomb, M.M. Denn, Flow of Bingham fluids in complex geometries, J. Non-Newton. Fluid Mech. 14 (1984) 337–346.
[12] D.N. Smyrnaios, J.A. Tsamopoulos, Squeeze flow of Bingham plastics, J. Non-Newton. Fluid Mech. 100 (1–3) (2001) 165–189.
[13] L. Muravleva, Squeeze plane flow of viscoplastic Bingham material, J. Non-Newton. Fluid Mech. 220 (2015) 148–161.
[14] J.G. Oldroyd, Two-dimensional plastic flow of a Bingham solid: A plastic boundary-layer theory for slow motion, Math. Proc. Camb. Phil. Soc. 43 (3) (1947) 383–395.
[15] G.H. Meeten, Effects of plate roughness in squeeze-flow rheometry, J. Non-Newton. Fluid Mech. 124 (1–3) (2004) 51–60.
[16] S.D.R. Wilson, Squeezing flow of a Bingham material, J. Non-Newton. Fluid Mech. 47 (1993) 211–219.
[17] I.A. Frigaard, D.P. Ryan, Flow of a visco-plastic fluid in a channel of slowly varying width, J. Non-Newton. Fluid Mech. 123 (1) (2004) 67–83.
[18] I. Walton, S. Bittleston, The axial flow of a Bingham plastic in a narrow eccentric annulus, J. Fluid Mech. 222 (1991) 39–60.
[19] N.J. Balmforth, R.V. Craster, A consistent thin-layer theory for Bingham plastics, J. Non-Newton. Fluid Mech. 84 (1) (1999) 65–81.
[20] A.R. Koblitz, S. Lovett, N. Nikiforakis, Viscoplastic squeeze flow between two identical infinite circular cylinders, Phys. Rev. Fluids 3 (2) (2018) 023301.
[21] K. Vajravelu, S. Sreenadh, V.R. Babu, Peristaltic transport of a Herschel–Bulkley fluid in an inclined tube, Int. J. Non-Linear Mech. 40 (1) (2005) 83–90.
[22] T. Hjelt, J.A. Ketoja, H. Kiiskinen, A.I. Koponen, E. Pääkkönen, Foam forming of fiber products: A review, J. Dispers. Sci. Technol. (2020) 1–37.
[23] V.J. Langlois, S. Hutzler, Dynamics of a flexible fibre in a sheared two-dimensional foam: Numerical simulations, Colloids Surf. A 534 (2017) 105–111.
[24] J. Lehmonen, E. Retulainen, J. Paltakari, K. Kinnunen-Raudaskoski, A. Koponen, Dewatering of foam-laid and water-laid structures and the formed web properties, Cellulose 27 (3) (2020) 1127–1146.
[25] O. Reynolds, IV. On the theory of lubrication and its application to Mr. Beauchamp Tower's experiments, including an experimental determination of the viscosity of olive oil, Philos. Trans. R. Soc. Lond. 177 (1886) 157–234.